2012

Divergent Functions of the Myotubularin (MTM) Homologs AtMTM1 and AtMTM2 in *Arabidopsis thaliana*: Evolution of the Plant MTM Family

Yong Ding
University of Nebraska-Lincoln, dingyong@ustc.edu.cn

Ivan Ndamukong
School of Biological Sciences, University of Nebraska–Lincoln

Yang Zhao
School of Biological Sciences, University of Nebraska-Lincoln

Yuannan Xia
Biotechnology Facility, University of Nebraska-Lincoln

Jean-Jack Riethoven
Center for Bioinformatics, University of Nebraska-Lincoln, jeanjack@unl.edu

See next page for additional authors

Published in *The Plant Journal* 70 (2012), pp. 866–878; doi: 10.1111/j.1365-313X.2012.04936.x

Submitted August 4, 2011; revised January 30, 2012; accepted February 3, 2012; published online March 30, 2012.

Supporting information for this article is available following the references.

Divergent Functions of the Myotubularin (MTM) Homologs AtMTM1 and AtMTM2 in *Arabidopsis thaliana*: Evolution of the Plant MTM Family

Yong Ding,[1*] Ivan Ndamukong,[1*†] Yang Zhao,[1*] Yuannan Xia,[2]

Jean-Jack Riethoven,[3] David R. Jones,[4] Nullin Divecha,[4]

and Zoya Avramova[1]

1. School of Biological Sciences, University of Nebraska at Lincoln, Lincoln, NE 68588, USA
2. Biotechnology Facility, University of Nebraska at Lincoln, Lincoln, NE 68588, USA
3. Center for Bioinformatics, University of Nebraska at Lincoln, Lincoln, NE 68588, USA
4. Inositide Laboratory, Paterson Institute for Cancer Research, University of Manchester, Manchester M20 4BX, UK

* These authors contributed equally to this work.
† Present address: Brody School of Medicine, Department of Microbiology and Immunology, East Carolina University, Greenville, North Carolina, 27834, USA

Corresponding author – Zoya Avramova, email zavramova2@unl.edu

Abstract
Myotubularin and myotubularin-related proteins are evolutionarily conserved in eukaryotes. Defects in their function result in muscular dystrophy, neuronal diseases, and leukemia in humans. In

contrast to the animal lineage, where genes encoding both active and inactive myotubularins (phosphoinositide 3-phosphatases) have appeared and proliferated in the basal metazoan group, myotubularin genes are not found in the unicellular relatives of green plants. However, they are present in land plants encoding proteins highly similar to the active metazoan enzymes. Despite their remarkable structural conservation, plant and animal myotubularins have significantly diverged in their functions. While loss of myotubularin function causes severe disease phenotypes in humans, it is not essential for the cellular homeostasis under normal conditions in *Arabidopsis thaliana*. Instead, myotubularin deficiency is associated with altered tolerance to dehydration stress. The two Arabidopsis genes *AtMTM1* and *AtMTM2* have originated from a segmental chromosomal duplication and encode catalytically active enzymes. However, only AtMTM1 is involved in elevating the cellular level of phosphatidylinositol 5-phosphate in response to dehydration stress, and the two myotubularins differentially affect the Arabidopsis dehydration stress-responding transcriptome. AtMTM1 and AtMTM2 display different localization patterns in the cell, consistent with the idea that they associate with different membranes to perform specific functions. A single amino acid mutation in AtMTM2 (L250W) results in a dramatic loss of subcellular localization. Mutations in this region are linked to disease conditions in humans.

Keywords: Arabidopsis MTM1, MTM2, plant myotubularins, evolution

Introduction

The myotubularin (MTM) and myotubularin-related (MTMR) proteins display the signature CX_5R motif of the members of the large family of dual-specificity serine-threonine phosphatase (DSP)-class I Cys-based protein tyrosine phosphatases (PTPs). However, they dephosphorylate lipids in vivo and have not been shown to dephosphorylate proteins (Blondeau et al., 2000; Taylor et al., 2000; Tronchère et al., 2004). The MTMs are phosphoinositide 3-phosphatases using phosphatidylinositol 3-phosphate (PtdIns3P) and phosphatidylinositol (3,5)-bisphosphate [PtdIns(3,5)P2] as substrates. Myotubularins carry the consensus sequence (CxDxxDR) at their catalytic site and utilize a unique mechanism during catalysis (Begley et al., 2003, 2006).

Despite being present at low levels in cells, regulated levels of PtdIns3P and PtdIns(3,5)P_2 are critical for cellular and organismal homeostasis (Michell et al., 2006). Using PtdIns(3,5)P_2 as a substrate MTMs can generate PtdIns5P, which until recently has been considered only as a source for the much more abundant PtdIns(4,5)P_2 (Rameh et al., 1997; Carlton and Cullen, 2005). However, research linking severe muscular and neurodegenerative diseases in humans with mutations in genes encoding PtdIns5P regulatory proteins has implicated PtdIns5P in these disease conditions. PtdIns5P is an intermediate in the cell osmoprotective response pathway (Sbrissa et al., 2002), in the etiology of severe muscular/neuronal pathologies, and in host-cell response to infection with the pathogen *Shigella flexneri* (Niebhur et al., 2002; Laporte et al., 2003; Pendaries et al., 2005). It is also implicated in the Akt pathway (Carricaburu et al., 2003; Pendaries et al., 2005; Coronas et al., 2007) and a role for PtdIns5P in regulating transport from late endosomal compartments to the plasma membrane of mammalian cells has been suggested (Lecompte et al., 2008).

Although the cellular localization and functions of PtdIns5P are still not well understood, its ability to bind the plant homology domain (PHD) of the tumor suppressor ING2

(inhibitor of growth family 2) to promote p53-dependent apoptosis under cellular stress (Gozani et al., 2004; Jones et al., 2006) has defined PtdIns5P as a ligand in nuclear signaling pathways (Jones and Divecha, 2004; Gozani et al., 2005).

All these mono- and bi-phosphorylated phosphoinositides have also been identified in plants and implicated in the responses to salinity, drought, temperature stresses or pathogenic invasion (reviews in Wang, 2004; Boss et al., 2006, Munnik and Vermeer, 2010; Vallutu and Van den Ende, 2011). Despite sharing common aspects, features unique to plants for PtdIns3P, PtdIns(3,5)P_2, and PtdIns5P signaling have been recognized. Phosphatidylinositol 3-phosphate modulates stomatal closing and actin reorganization in guard cells (Jung et al., 2002; Choi et al., 2008) and might mediate oscillations in Ca^{2+} levels (Jung et al., 2002) as well as the generation of reactive oxygen species (ROS) in response to abscisic acid (Park et al. 2003). The function of PtdIns(3,5)P_2 in plants is still completely unknown except for its accumulation in cells under hyperosmotic stress, suggesting a role in the water stress response (Meijer and Munnik, 2003; Zonia and Munnik, 2004).

Plants contain only trace amounts of PtdIns5P, but elevated PtdIns5P has been reported within minutes of salt stress in *Chlamydomonas* and in cultured carrot cells, as well as in tomato, pea, and alfalfa plant tissues (Meijer et al., 2001). Transcriptome analysis has revealed that PtdIns4P and PtdIns5P trigger distinct specific responses of *Arabidopsis thaliana* genes (Alvarez-Venegas et al., 2006a). However, studies of PtdIns5P in plants have been hampered by its low endogenous levels under non-stressed conditions and by the difficulty in separating PtdIns5P from PtdIns4P by either TLC or HPLC (Pical et al., 1999; Meijer et al., 2001; Ndamukong et al., 2010). Using a radioactive mass assay (Jones et al., 2009), we have positively identified PtdIns5P in *A. thaliana* cells and have demonstrated that endogenous PtdIns5P increases upon both dehydration and hypotonic stresses (Ndamukong et al., 2010). The ARABIDOPSIS HOMOLOG OF TRITHORAX 1 (ATX1) specifically binds PtdIns5P through its PHD domain. The ATX1 protein is a histone modifier responsible for the histone H3 lysine 4 trimethylation (H3K4me3) of its target genes, a modification linked to actively transcribed genes (Avramova, 2009; Cazzonelli et al., 2009). Elevated PtdIns5P negatively affects ATX1 activity at a co-regulated set of genes (Alvarez-Venegas et al., 2006b) by restricting access of ATX1 to chromatin (Ndamukong et al., 2010).

The emergence of PtdIns5P as a messenger in a signaling pathway that links lipid signaling with chromatin (epigenetic) regulation in plant cells underlies our interest in activities generating cellular PtdIns5P. The canonical pathway to its production is through dephosphorylation of PtdIns(3,5)P_2 by the MTMs (Tronchère et al., 2004; Ding et al., 2009). Two other phosphatases can produce PtdIns5P from PtdIns(4,5)P_2 (Ungewickell et al., 2005) in human cells, but this route is thought to be exclusive to metazoans (Lecompte et al., 2008).

Myotubularins form a family of about 15 members in humans (Vergne and Deretic, 2010). A remarkable feature is that about half of the family members have conserved mutations in the amino acids in the catalytic site rendering them enzymatically inactive. Inactive MTMs also have physiological roles, most likely as regulators of the active enzymes (Begley and Dixon, 2005). Inactive MTMs are found early in eukaryotic evolution, present in multicellular as well as unicellular forms of life, like *Dictyostelium discoideum*, *Entamoeba histolytica*, and *Monosiga brevicollis* (Kerk and Moorhead, 2010). The catalytically active

MTMs show identical substrate specificity in vitro, high sequence homology (especially within a subgroup) and an overall ubiquitous expression, but, nonetheless, loss-of-function of a particular MTM leads to specific disease phenotypes indicating that they possess specific roles. Thus, mutations in MTM1 lead to myotubular myopathy, a severe X-linked congenital myopathy characterized by the abnormal positioning of nuclei within muscle fibers (Laporte et al., 1996), while mutations in the highly similar MTMR2 affect the peripheral nervous system causing the Charcot–Marie–Tooth neuropathy type 4B1 (CMT4B1) (Bolino et al., 2000; Kim et al., 2002).

Despite the high evolutionary conservation of the MTM-encoding genes in metazoans and in plants their functions have greatly diverged. Plants do not encode inactive MTMs (see further below) and it is impossible to predict a role for the plant homologs based on the phenotypes (muscular dystrophy, neuronal malfunction, and leukemia) caused by MTM mutations in humans. Two genes, *ARABIDOPSIS MYOTUBULARIN1* (*AtMTM1*) and *ARABIDOPSIS MYOTUBULARIN2* (*AtMTM2*), originating from a segmental chromosomal duplication encode MTM homologs in Arabidopsis. Structurally, the genes are highly similar with conserved biochemically active catalytic sites. According to current theoretical models, the two genes may either have redundant functions or may have entered a path of divergence that could lead to subfunctionalization (Kondrashov et al., 2005). Here, we analyze the functions of the two genes in parallel and demonstrate that AtMTM2, in contrast to AtMTM1 (Ding et al., 2009; Ndamukong et al., 2010), is not involved in the plant's resistance to dehydration stress and is not essential for the endogenous elevation of PtdIns5P under dehydration stress. In addition, AtMTM1 and AtMTM2 display different affinities for the two common substrates, show different distribution patterns in the cell and differentially affect the Arabidopsis dehydration stress-responding transcriptome.

Thereby, despite preserving identical catalytic sites and largely overlapping domains of expression in the plant, the two genes have functionally diverged, suggesting that each gene has evolved along a different evolutionary path. The evolution of the MTM genes in the plant lineage is also analyzed.

Results

Origin of the two Arabidopsis MTM genes

The *A. thaliana* genes *At3g10550* and *At5g04540* (named *AtMTM1* and *AtMTM2*, respectively), encode myotubularin (AtMTM) homologs (Fig. 1a). The two proteins are 77% identical, 85% similar to each other and to the human MTMR2 (34% identical, 49% similar, 4×10^{-81}). The proteins contain a conserved PH-GRAM domain, found in a number of membrane-interacting proteins, a putative membrane-targeting motif (RID, the Rac-induced recruitment domain), as well as the catalytic domain and the SET-interacting domain (SID) (Laporte et al., 2002; Begley et al., 2003). The PTP/DSPs catalytic domains carry the consensus motif of DSP-class I-phosphatases, but the unique presence of the SID and the RID motifs is a signature feature for the MTMs.

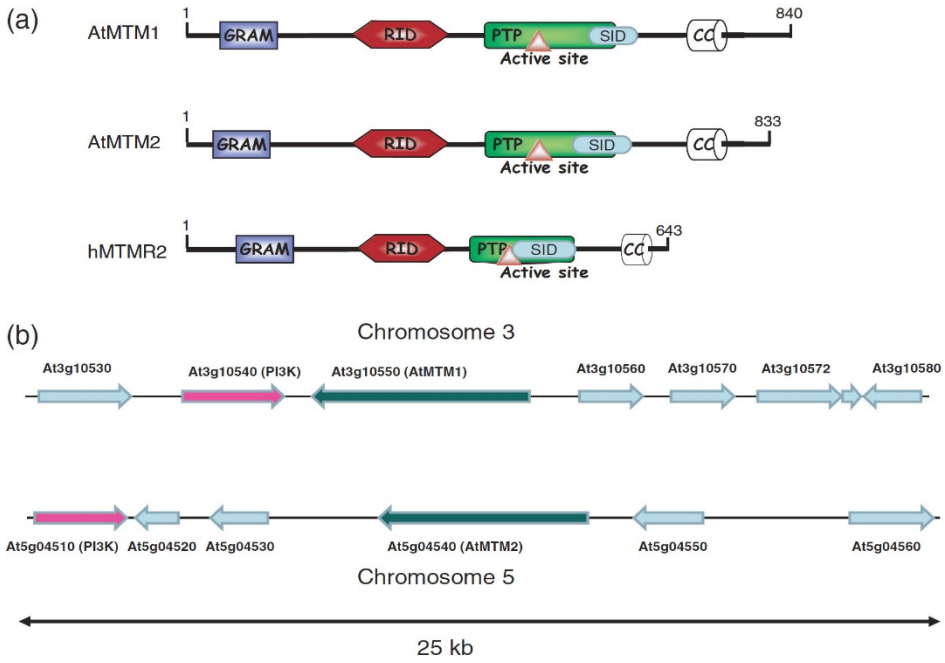

Figure 1. Structure of the *Arabidopsis thaliana* myotubularins AtMTM1 and AtMTM2, showing segmental duplication of the *At3g10550* and *At5g04540* gene containing regions on chromosomes 3 and 5. (a) Structures of AtMTM1 and AtMTM2 and of the human homolog hMTMR2. The conserved domains, GRAM (glycosyltransferase, Rab-like GTPase activator and myotubularins), RID (Rac-induced membrane-binding domain), the phosphatase (PTP) region with the catalytically active sites and SID (the SET-interacting domain) are indicated. The Arabidopsis and the human myotubularins contain predicted coil-coil (CC) domains, albeit the sequences are not as highly conserved between the plant and the human proteins. (b) Locations of the *At3g10550* and *At5g04540* genes on chromosomes 3 and 5, respectively. The genes encoding conserved 3′-PIP-dependent kinases are shown in pink. Shaded areas illustrate conserved DNA sequences on the two chromosomes. The two genes between the *AtMTM2* and the 3′-PtdInsP-dependent kinase on chromosome 5 (*At5g04530* and *At5g04520*) encode a KCS19 (3-ketoacyl-CoA synthase19) and a hypothetical protein, respectively.

Detailed analysis of the locations of *At3g10540* and *At5g04510* genes on chromosomes 3 and 5, respectively, indicated that a relatively small region encompassing the *AtMTM* gene and a downstream gene encoding a 3′-phosphatidylinositol phosphate-dependent kinase is conserved on both chromosomes. The *At3g10540* gene is adjacent to *AtMTM1*, while *At5g04510* is positioned two genes downstream of *AtMTM2* on chromosome 5 (Fig. 1b). The results illustrate a segmental chromosomal duplication of the DNA regions involving the *AtMTM1*/*AtMTM2* genes and the neighboring sequences encoding a kinase using the same substrate, PtdIns3P.

Duplicated genes may remain as redundant functions or may evolve along separate paths to adapt for different functions. The fate of the duplicated phosphoinositide 3-phosphatase genes in Arabidopsis was analyzed next.

Domains of AtMTM1 *and* AtMTM2 *expression in* A. thaliana

Transgenic lines expressing the β-glucuronidase (GUS) coding sequence under the *AtMTM1* or *AtMTM2* promoters (see Experimental procedures) were generated, and a dozen independently transformed lines (for each *AtMTM1* and *AtMTM2*) were examined for GUS expression at different developmental stages. By being expressed in different temporal and/or spatial manners, redundant genes may acquire functional divergence (Pickett and Meeks-Wagner, 1995).

Overall, the promoters of both genes outlined similar domains of expression activity (Fig. 2a). Young seedlings displayed very strong staining throughout, and at the tip of the growing shoot meristems in particular. Later in development, expression was observed in roots and in aerial parts. The staining intensity was disperse and weak in the rosette leaves but remained well pronounced in the trichomes and in cotyledon veins. The staining in the flowers was also weak, but strong staining was displayed in cells at organ-stem junctions (Fig. 2a). In particular, the activity of the *AtMTM2* promoter was restricted to the developing peduncle (Fig. 2a, arrows), while active *AtMTM1* promoter domains were diffuse, appearing as patches along the stem but also concentrated at the peduncle. We note the activity of the *AtMTM1* promoter in the septum and the funiculi of the developing siliques (Fig. 2a).

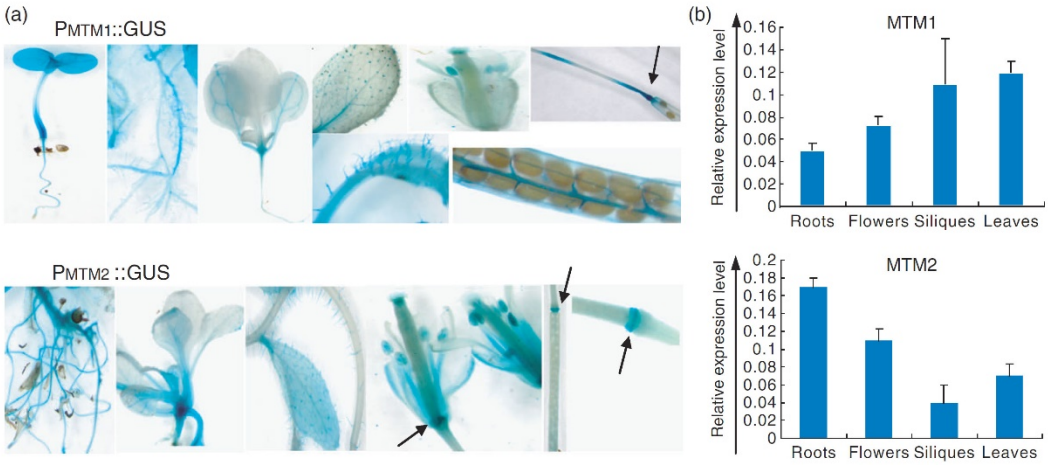

Figure 2. Domains of *AtMTM1* and *AtMTM2* expression in Arabidopsis plants. (a) Transgenic lines expressing the β-glucuronidase (GUS) coding sequence under the promoters for the *AtMTM1* (P_{MTM1}::GUS) or *AtMTM2* (P_{MTM2}::GUS) genes, respectively. Arrows point to peduncle cells. Specific expression of P_{MTM1}::GUS in the septum and funiculi of developing siliques (see text). (b) Tissue-specific *AtMTM1* and *AtMTM2* expression. The mRNA levels are measured by real-time quantitative RT-PCR. Bars are standard deviations from three independent measurements.

Collectively, GUS staining suggested largely overlapping expression patterns for the *AtMTM1* and *AtMTM2* genes *in planta*. However, as transgenic GUS expression reflects not only the strength of the promoters but is also dependent on the sites of insertion and on effects of potential regulatory sequences located in introns, we analyzed the mRNA levels of *AtMTM1* and *AtMTM2* by real-time quantitative PCR (qPCR) (Fig. 2b). The results confirmed that *AtMTM1* and *AtMTM2* were ubiquitously expressed. However, in mature plants higher *AtMTM1* transcripts were found in leaves and siliques, while *AtMTM2* transcript levels were more abundant in the roots (Fig. 2b). The tissue-specific intensity of each gene's expression suggested that *AtMTM1* and *AtMTM2* were differentially regulated in specific cell types.

AtMTM1 and AtMTM2 expression in response to dehydration

Our earlier studies implicated AtMTM1 in the Arabidopsis response to dehydration stress (Ding et al., 2009; Ndamukong et al., 2010). Whether AtMTM2 was involved was examined by quantitative qRT-PCR assays of *AtMTM2* mRNAs produced under both watered and dehydration stress conditions (see Experimental procedures). In contrast to *AtMTM1*, the *AtMTM2* transcripts did not increase during dehydration stress (Fig. 3a). Increased expression in hydathodes of P_{AtMTM1}::GUS, but not of P_{AtMTM2}::GUS (Fig. 3b) illustrates cell-specific activation of the *AtMTM1* promoter upon dehydration stress.

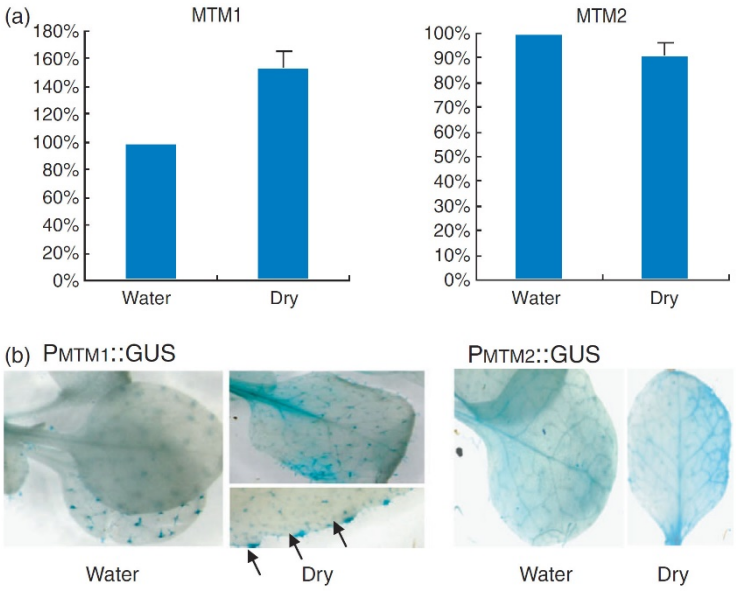

Figure 3. Expression of *AtMTM1* and *AtMTM2* in response to dehydration stress. (a) Relative *AtMTM1* or *AtMTM2* transcripts under non-stressed (water) and stressed (dry) conditions quantified by real-time PCR shown as a percentage of the non-stressed watered levels. Bars are standard deviations from three independent measurements. (b) Activity of the *AtMTM1* or *AtMTM2* promoters under watered or dry conditions, respectively. Increased expression of PAtMTM1::GUS upon dehydration stress in hydathodes (indicated by arrows).

Loss of AtMTM1 and AtMTM2 functions in mtm1 and mtm2 mutant plants

Whether the high structural similarity between *AtMTM1* and *AtMTM2* resulted in functional redundancy was examined in *Ti*-insertion lines (see Experimental procedures). Among the seven available lines only three germinated successfully and contained the expected *Ti*-insertions: SALK_029185, SALK_073312 (referred to as *mtm1-1* and *mtm1-2*, respectively), and SALK_147282 (*mtm2*) (SF1 A). Homozygous mutant lines were selected, verified by genotyping, and tested for producing mRNAs (specific primers are shown in Table S1 in the Supporting Information).

No full-size *AtMTM1*mRNA was detected in the *mtm1-1* or *mtm1-2* backgrounds, but low-level *AtMTM1m*RNA was produced in the SALK_073312 line (*mtm1-2*) containing a *Ti*-DNA insertion in the 3′ untranslated region (UTR) (SF1B). No *AtMTM2m* RNA was detected in the SALK_147282 line. Importantly, the *AtMTM1* expression in the *mtm2* mutant background and of *AtMTM2* in *mtm1-1* and *mtm1-2* backgrounds were similar to their respective levels in the wild type (Col-0), indicating that the *AtMTM1* and *AtMTM2* genes did not influence each other's transcriptional behavior.

Plants were grown under normal conditions and scored for possible deviations from the wild type. No phenotypes were detected in any mutant line from germination to seed-producing stages under greenhouse conditions (12 h light, 20°C, regular watering). Given that no transcripts were produced in the *mtm2* and *mtm1-1* backgrounds, these mutants were considered null. Lack of a phenotype, therefore, suggested functional redundancy for *AtMTM1* and *AtMTM2*, a possibility that was further explored.

Responses to soil-water-withdrawal dehydration stress

The different transcriptional responses from the *AtMTM1* and *AtMTM* genes during dehydration stress suggested that *mtm1* and *mtm2* mutant plants might show different sensitivity to dehydration. Three-week-old Col-0 and homozygous *mtm1-1*, *mtm1-2*, and *mtm2* plants were tested for their resistance to soil-water withdrawal. After 19 days without watering, the Col-0 plants were severely dehydrated, while the *mtm1-1* mutants displayed increased resistance (Fig. 4). The response of the *mtm2* plants was similar to the Col-0 plants, illustrating a major contrast with *mtm1-1* mutants.

The different involvement of the two genes in the dehydration stress response was further confirmed by generating and testing double mutants. The double *mtm1-1*$^{-/-}$/*mtm2*$^{-/-}$ mutants showed stress resistance similar to the single *mtm1-1* mutants (Fig. 4). We conclude that loss of *AtMTM1* function, but not of *AtMTM2*, conferred increased resistance to soil-water-deficit stress. However, neither the *mtm1-2* mutants nor the *mtm1-2*/*mtm2* mutants showed responses significantly different from the wild type (*SF 2*) and were not included in subsequent studies.

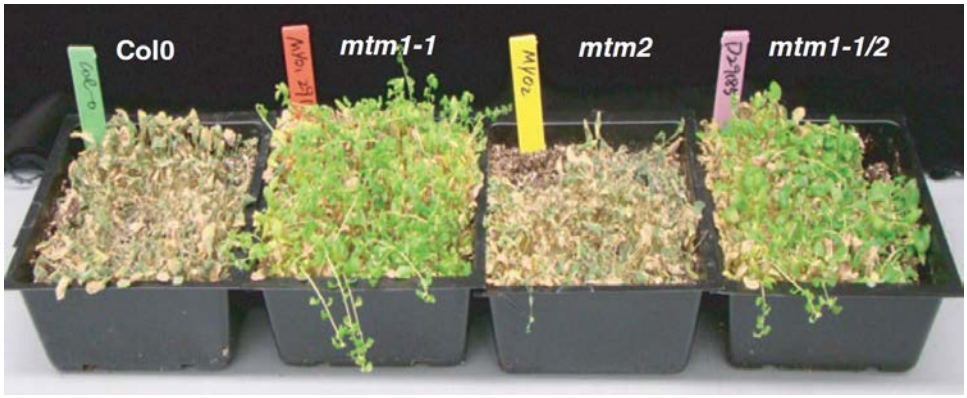

Figure 4. Responses to soil water-withdrawal stress of plants from different genetic backgrounds. Plants from the wild type (Col-0) and from the homozygous *mtm1-1*, *mtm2*, and *mtm1-1*/*mtm2* backgrounds after 19 days without watering.

Differential roles of AtMTM1 *and* AtMTM2 *at the genome level*

To distinguish the roles of *AtMTM1* and *AtMTM2* at the global genome level, we performed transcription profiling in the *mtm1* or *mtm2* backgrounds under non-stressed and during dehydration stress conditions. We assumed that AtMTM1 and AtMTM2 participate in pathway(s) that transfer gene regulatory signals to the nucleus and do not imply that AtMTM1 or AtMTM2 directly regulate gene expression. Cluster (overlap) analyses are among the best available tools for outlining common, or partially overlapping, pathways. Largely overlapping gene sets from the *mtm1* and *mtm2* data would be consistent with redundant *AtMTM1* and *AtMTM2* functions. The gene expression data are interpreted within this context.

Affymetrix gene chips (ATH1 Genome Arrays, with ~24 000 Arabidopsis genes) were used in whole-genome expression analysis of *mtm1-1* and *mtm2* homozygous mutant plants. The RNA was isolated from rosette leaves of 3-week-old mutant and Col-0 plants in two independent biological replicates. Plants from the respective backgrounds grown under watered conditions were used as controls for dehydration-stressed plants. These experiments were performed as part of a larger experiment involving two additional mutant backgrounds (*atx1* and *OX-AtMTM1* plants). Detailed conditions and microarray data analyses and validation have already been published (Ding et al., 2009; see also Experimental procedures).

Under watered conditions, 27 genes significantly changed expression in the *mtm1* background, while none changed expression in *mtm2* background (ST 2). After dehydration stress, transcripts of 134 genes in *mtm1* plants deviated significantly (73 up-regulated, 61 down-regulated) from the dehydration-stressed Col-0 plants. The majority of these genes included biotic, abiotic, and heat shock stress-response genes (26 genes) and transcription factors (23, six belonging to the Myb family), in addition to metabolic and membrane-wall associated functions (ST 3). In contrast, only four genes were differentially expressed (down-regulated) in the stressed *mtm2* plants: three of these four genes were also present

in the down-regulated *mtm1* fraction including the *ACS7* gene (*At4g26200*) involved in ethylene biosynthesis and in responses to abscisic acid (ABA) (Wang et al., 2005), a gene (*At2g02060*) encoding a transcription factor from the Myb family, and the *At5g12030* gene encoding a cytosolic small heat shock protein with chaperone activity that is induced by heat and osmotic stress. The fourth gene identified in the *mtm2* deregulated gene-set was the *AtMTM2* gene, capturing the lost signal from *AtMTM2* transcripts in the SALK_147282 (see Fig. S1b).

Collectively, the results illustrated differential roles for AtMTM1 and AtMTM2 in the dehydration stress-responding transcriptome in *A. thaliana*, suggesting that AtMTM1 and AtMTM2 participate in separate cellular signaling pathways.

Contributions by AtMTM1 and AtMTM2 to the endogenous PtdIns5P pool

To determine whether the lesser involvement of AtMTM2 in the dehydration stress response influenced the endogenous PtdIns5P level in Arabidopsis cells differently from AtMTM1 during the response to dehydration stress, we quantitatively determined PtdIns5P, as previously described (Jones et al., 2009; see Supplementary Methods for details).

Under non-stressed (watered) conditions, the loss of AtMTM2-function did not significantly affect the PtdIns5P level in *mtm2* mutant cells. Upon dehydration, PtdIns5P in the *mtm2* background increased to a degree comparable to the wild-type cells, indicating that AtMTM2 depletion did not significantly affect the production of PtdIns5P (Fig. 5). Thereby, loss of MTM2 function did not cause a response different from the wild type. Statistical analysis by a two-way ANOVA (ANOVA-N) confirmed no difference in the stress responses of *mtm2* and wild type ($P = 0.3064$). In contrast, *mtm1* mutant cells showed lack of PtdIns5P increase in response to dehydration. The difference in PtdIns5P production in wild-type and *mtm1* mutant cells under stress is significant ($P = 0.0185$), indicating that AtMTM1 mediates the increase in PtdIns5P during the response to dehydration stress. These results are in full agreement with our earlier results showing that AtMTM1 overexpression elevated the endogenous PtdIns5P (Ndamukong et al., 2010). Neither MTM was affecting the low basal level of endogenous PtdIns5P in hydrated cells. However, their differential involvement in PtdIns5P levels under dehydration stress provided strong evidence that AtMTM1, but not AtMTM2, function was required for the PtdIns5P response. The question of whether AtMTM2 has preserved its enzyme activity was explored next.

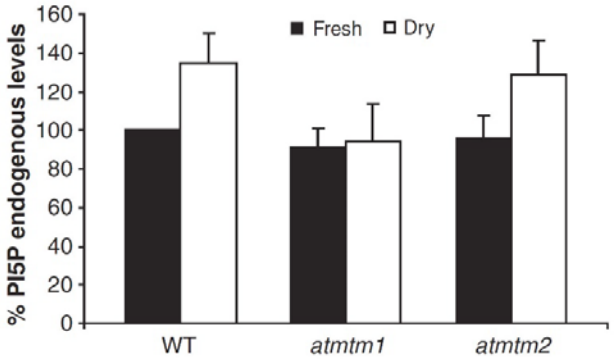

Figure 5. Contributions by AtMTM1 and AtMTM2 to the cellular phosphatidylinositol 5-phosphate (PtdIns5P) level. The PtdIns5P levels in the wild type (WT) (Col-0) and in homozygous mutant *mtm1* or *mtm2* plants under non-stressed (black columns) or after dehydration stress conditions (white columns). Data are expressed as mean ± SD. Statistical analysis by a two-way ANOVA (ANOVA-N) confirmed no difference in the stress responses of *mtm2* and the wild type ($P = 0.3064$); the difference in PtdIns5P production in wild-type and *mtm1* mutant cells under stress is significant ($P = 0.0185$).

Phosphatase activities of AtMTM1 *and* AtMTM2

The RID, the PTP/DSPs and SID define the catalytic domain of MTMs, and all essential amino acids determined to be critical for MTMR2 function (Begley et al., 2003; Robinson and Dixon, 2006) are conserved in the two Arabidopsis homologs. AtMTM1 has 3′-phosphatase activity with both PtdIns3,5P_2 and PtdIns3P substrates (Ding et al., 2009). Here, we determined that AtMTM2 was also catalytically active. A recombinant glutathione *S*-transferase (GST)-tagged construct containing the AtMTM2 RID-PTP-SID domain regions was tested for enzyme activity by the malachite green assay (Martin et al., 1985; Schaletzky et al., 2003). A recombinant GST-tagged AtMTM1 protein expressed, purified and tested in parallel was used as a positive control. The kinetic parameters of the phosphatase activity of both AtMTM1 and AtMTM2 were measured with both substrates. Based on the Lineweaver-Burk curves (Fig. 6a–d), for AtMTM2 we estimated a slightly higher affinity (K_m = 158.2 μM) and activity (V_{max} = 28.4 pmol min^{-1} mg^{-1}) with Ptdins3,5P_2 than with Ptdins3P (K_m = 216.5 μM, V_{max} = 15.4 pmol min^{-1} mg^{-1}). A preference for Ptdins3,5P^2 as a substrate versus Ptdins3P was also shown by AtMTM1 (K_m = 146 μM and V_{max} = 142.6 pmol min^{-1} mg^{-1} with Ptdins3,5P_2; K_m = 201.7 μM and V_{max} = 94.3 pmol min^{-1} mg^{-1} with Ptdins3P). Thereby, AtMTM2 is a catalytically active phosphatase that shows similar substrate-binding specificity as AtMTM1 (the K_m values for each substrate are comparable for the two enzymes). Important differences, however, are the lower dephosphorylation rates of both substrates by AtMTM2 compared with AtMTM1 (Fig. 6e). Thereby, although enzymatically active AtMTM2 shows a much lower activity than AtMTM1.

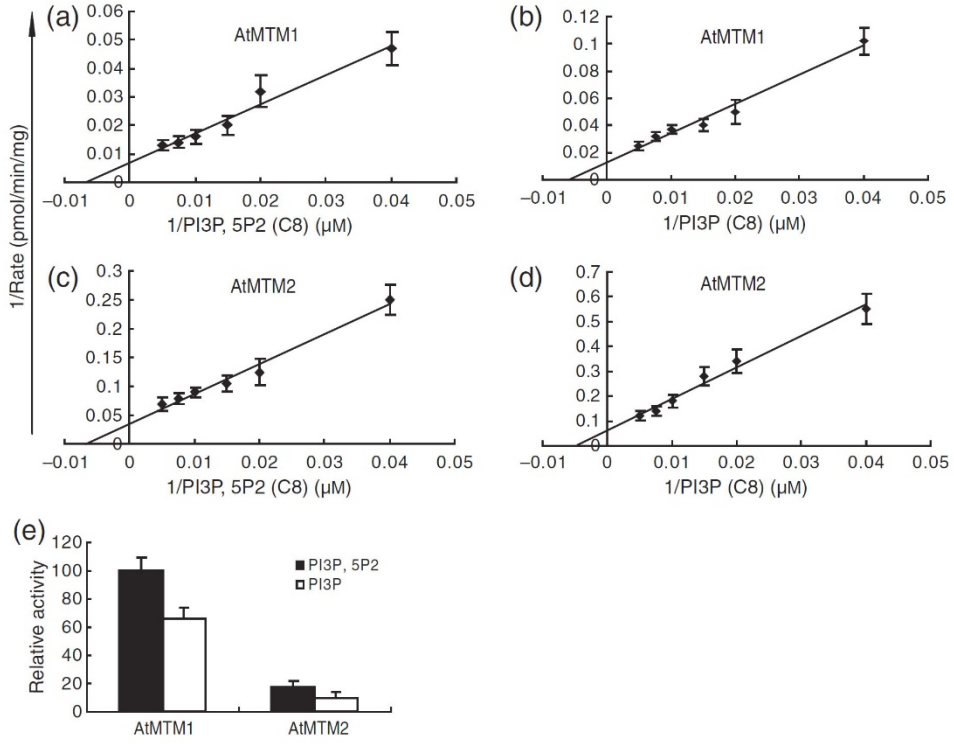

Figure 6. Enzyme activities of AtMTM1 and AtMTM2 with phosphatidylinositol (3,5)-bisphosphate [PtdIns(3,5)P_2] and phosphatidylinositol 3-phosphate (PtdIns3P) substrates. Phosphoinositide 3′-phosphatase activity of the two proteins with PtdIns3P and PtdIns(3,5)P_2 as substrates. (a–d) Lineweaver-Burk curves for PtdIns(3,5)P_2 and PtdIns3P used as substrates with AtMTM1 (a, b) and with AtMTM2 (c, d). See text for kinetic parameters. (e) Relative activity of AtMTM2 with both substrates versus AtMTM1.

Subcellular localization

Next, we compared the subcellular localization of the two plant MTMR proteins. Fluorescently-tagged tMTM1 is seen mostly as granular particles of varying abundance and size at the cell periphery and throughout the cytoplasm (Fig. 7a). This AtMTM1 distribution pattern is highly reproducible, as we have seen in our earlier studies (Ndamukong et al., 2010). The nature of these particulate structures remains unclear but, interestingly, cytoplasmic "punctate elements" of unknown origins have also been reported for mammalian MTMs (Kim et al., 2002; Laporte et al., 2002; Nandukar et al., 2003).

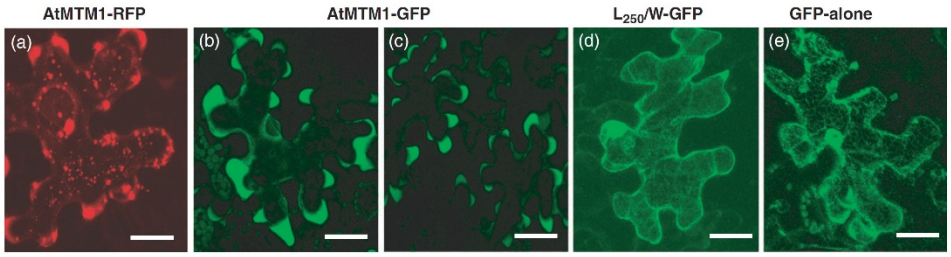

Figure 7. Subcellular localization of fluorescently tagged Arabidopsis myotubularins (MTMs). (a) Red fluorescent protein (RFP)-AtMTM1 fusion protein expressed in tobacco cells associated with numerous granular structures. (b, c) GFP-tagged AtMTM2 expressed in tobacco cells seen under different exposures. The strongly concentrated signal localizes at the cell periphery. No particulate structures were seen associated with AtMTM2. (d) An altered AtMTM2-GFP distribution of the L250W AtMTM2-GFP construct. (e) Distribution of a control (empty) GFP. Bars are 20 nm.

A GFP-AtMTM2 fusion protein transiently expressed in tobacco leaf cells displayed a visibly different distribution pattern: a diffuse green signal appeared throughout the cytoplasm but the signal was highly concentrated at the peripheral lobes of the epidermal cells (Fig. 7b,c). Interestingly, no granular particulate structures were observed in AtMTM2 in transformed cells, suggesting that AtMTM1 and AtMTM2 associate with different substructures inside cells.

Loss of AtMTM2 subcellular localization resulting from a single amino acid mutation

One of our AtMTM2-GFP constructs showed a different intracellular distribution similar to the distribution of GFP alone (Fig. 7d,e). The signal distribution suggested to us that AtMTM2 in this particular construct had lost its usual localization in the dense regions at the periphery. The subsequent sequencing of the construct revealed a single amino acid substitution (L250W). This mutation appears to be linked to this different localization and/or a lost ability of AtMTM2 to associate with specific cellular substructures.

Evolution of plant MTMs

Myotubularin-encoding genes have proliferated in the animal lineage as five copies have been identified in the genome of the unicellular metazoan relative *M. brevicollis* (Kerk and Moorhead, 2010). Interestingly, there are no MTMR genes in the genomes of the green algae, including *Chlamydomonas*, which shares a common ancestor with green plants (Merchant et al., 2007; Herron et al., 2009). To trace the evolution of MTM genes in the plant lineage, we analyzed several fully sequenced plant genomes.

The moss *Physcomitrella patens* is an extant relative of the earliest land plants considered half-way between algae and angiosperms (Quatrano et al., 2007). The lycophyte *Selaginella moellendorffii*, with no true roots and leaves, occupies an important node in the plant evolutionary tree (Hedges et al., 2004). There are two MTM-type genes in the genome of the moss (Kerk and Moorhead, 2010) while one, weakly related, gene in *Selaginella* is fused with additional domains not found in any other known myotubularin (*SF 3*). The two

Physcomitrella myotubularins have similar structures to the animal and plants proteins. The C-terminal regions of the moss proteins, however, are only weakly related to the coil-coil domain sequences of the other MTMs and belong to the Flagellar family of proteins found in eukaryotic paraflagellar rod component proteins. The moss proteins are most highly related to each other, suggesting that the two copies have resulted from moss-specific gene duplication. Different genes flank the MTM gene on the respective chromosomes restricting the duplication to the MTM sequence.

There is only one copy of a MTM-encoding gene in the genomes of mono- and dicotyledonous plants tested here, with the notable exception of Arabidopsis (see above). The gene encoding a MTM in rice (*Os08g05567*) is homologous to two adjacently positioned genes (SORDIDRAFT_07g024440 and SORDIDRAFT_07g024450) on the sorghum chromosome, encoding the N-terminal and C-terminal halves of the MTM protein. Together, the two genes encode a full-length MTM, highly related to the rice and to all plant MTMs. Distribution of the coding sequences into two sorghum genes, thereby, might reflect an annotation problem. The chromosomal regions upstream of the rice and sorghum MTM genes are divergent, sharing only one common gene. However, there is a remarkable collinearity of the regions downstream of the MTM genes conserved in the evolution of the two grass genomes (Fig. 8a).

As in monocots, single genes encode MTM homologs in representatives of the eudicots, *Populus trichocarpa* (poplar), *Vitis vinifera* (grapevine), and *Ricinus communis*. Analyses of the poplar and the grapevine genomes have suggested that these species have captured traits common to all eurosids (Tuskan et al., 2006; Jaillon et al., 2007). Furthermore, the collinearity downstream from the respective MTM gene is well preserved between the chromosomes of these three species (Fig. 8b). The need to thrive in fixed locations over centuries under changing environmental conditions and biotic and abiotic stresses sets these species apart from the shorter-lived herbaceous (*Ricinus* and *Arabidopsis*) plants.

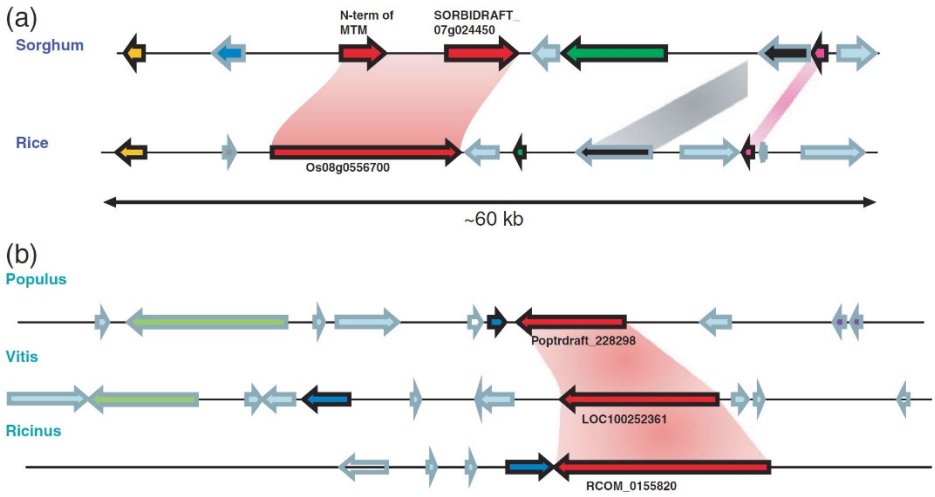

Figure 8. Collinearity of the myotubularin (MTM) gene-containing regions in plants. (a) Single copies of myotubularin-encoding genes are found in largely collinear regions (shaded area) on the sorghum and rice chromosomes. The two adjacent genes (SORDIDRAFT_07g024440 and SORDIDRAFT_07g024450) on the sorghum chromosome encode the N-terminal and C-terminal halves of the myotubularin protein. The collinearity here also extends to regions upstream of the myotubularin gene including a gene for a putative Peptidase_C1A protein. Homologous genes at the collinear regions are shown in the same colors. (b) Single genes encode myotubularin homologs in genomes of the dicotyledonous *Populus trichocarpa*, *Vitis vinifera*, and *Ricinus communis*. Collinearity downstream from the respective myotubularin gene is well preserved between the chromosomes of the three species. No data are available for the genes in the neighborhood of the myotubularin gene in *Ricinus* preventing a more extended analysis of the chromosomal region. Homologous genes at the collinear regions are shown in the same colors.

Discussion

The *A. thaliana* MTM genes *AtMTM1* and *AtMTM2* have originated from a segmental duplication involving the MTM-encoding and the adjacent PIP3K-encoding sequences on chromosomes 3 and 5. Accordingly, the two *A. thaliana* MTMs are most highly related among themselves. Analysis of the MTM-related genes in the closely related *Arabidopsis lyrata* revealed that homologs of both *AtMTM1* and *AtMTM2* genes are present in conserved collinear regions in the respective chromosomes. The two Arabidopsis species split about 13 million years ago (Beilstein et al., 2010) and the conserved gene duplication and collinearity that are different from the collinear regions in *Populus*, *Vitis*, and *Ricinus* suggests that the duplication and rearrangement at the MTM locus occurred after separation of the Arabidopsis lineage from the other dicots. The collinearity downstream of the single sorghum and rice MTM genes (Fig. 8a), as well as the extended collinear regions containing the myotubularin genes in *Populus*, *Vitis*, and *Ricinus* (Fig. 8b) illustrate a remarkably stable arrangement of these regions inherited from the ancestral monocot or dicot chromosomes, respectively.

Plants do not carry genes encoding inactive MTMs. In contrast, genes encoding both active and inactive MTMs have proliferated in the basal metazoan group. There are five genes in *M. brevicollis* and eight in *Trichoplax adhearens* (Kerk and Moorhead, 2010). It is quite surprising, then, that in species ancestral to the green plants (*Chlamydomonas reinhardtii*, *Volvox carterii*, *Ostreococcus tauri*, *Ostreococcus lucimarinus*) there are no MTM-related genes. However, the appearance of MTM-encoding genes in the moss suggests that a primordial gene present in the last eukaryotic ancestor (LECA) has been lost at the separation of the algal lineages but has survived in the ancestor of the extant green plant lineage. Furthermore, in the moss and in Arabidopsis the MTM gene has undergone species-specific duplications.

Despite the high degree of structural similarity between the MTMs from animal and plant origins, the genes in each lineage have evolved along different paths and the encoded proteins have acquired distinct functions. The different requirements for MTM activities in the plant and animal systems is illustrated by our results here, showing that, in contrast to MTM deficiency in humans (Laporte et al., 2003; Pendaries et al., 2005), loss of MTM function does not cause severe phenotypes in Arabidopsis under regular, nonstressed, conditions.

Recognized as a force in the evolution of biological diversity, duplicated genes may remain as redundant functions or may acquire specialized roles. In contrast to single copies in angiosperms, there are two Arabidopsis genes that have diverged in function. The following results support this conclusion: First, despite being expressed in the same tissues, *AtMTM1* and *AtMTM2* mRNAs display tissue-specific accumulation (Fig. 2a,b). Second, *AtMTM1* and *AtMTM2* show distinct transcriptional responses and different roles in the response to drought exposure (Figs. 3a and 4). The higher resistance of *mtm1* mutants to water-withdrawal stress is mirrored by the decreased resistance of plants overexpressing AtMTM1 (Ding et al., 2009) providing independent support to the conclusion that AtMTM1 is involved in the dehydration stress response in Arabidopsis. One possible scenario is through effects on the endogenous PtdIns3P levels, which was shown to stimulate stomatal closures (Choi et al., 2008). Third, critical evidence for functional divergence between *AtMTM1* and *AtMTM2* emerged from the transcriptome analysis of the respective mutants under watered and dehydration stress conditions. While AtMTM1 loss of function affected transcription from 134 dehydration-response genes, only three genes were misregulated in *mtm2* cells. These results are important, as they illustrate very different roles at the global genome level. Fourth, different contributions of AtMTM1 and AtMTM2 to the endogenous PtdIns5P level provided yet further evidence for distinct functions: in contrast to AtMTM2, only AtMTM1 significantly affected the cellular PtdIns5P level under dehydration stress (Fig. 5). Both Arabidopsis proteins are enzymatically active, but the lower AtMTM2 activity (Fig. 6a–e) could account partially for this result. Lack of *AtMTM2* induction by dehydration stress is another factor. It will be interesting to establish whether *AtMTM2* transcription would be stimulated by a different type of a stress. Different PtdIns5P levels produced under stress could be related with an association of AtMTM1 and AtMTM2 with different subcellular membranes so that each phosphatase could be accessing and working on different lipid pools. This possibility has been used to explain

the unique functional roles of human MTMs despite identical (in vitro) substrate specificity, sequence homology and ubiquitous expression (Pendaries et al., 2003; Laporte et al., 2003; Cao et al., 2008). Their highly specific roles are thought to be determined by the nature of the membranes they are attached to and by the nature of the phosphoinositide anchored on specific membranes, as PtdInsP isomers are viewed as docking sites that "attract" signaling proteins to specific membranes "guiding" them to their substrates (Robinson and Dixon, 2006). In plants, a phosphoinositide transiently increasing under hyperosmotic stress represents a physiological pool different from the constitutive phosphoinositide pools of nonchallenged plants (König et al., 2007), and thus stress-inducible and constitutive phosphoinositide pools may involve different enzyme activities (König et al., 2007, 2008). Fifth, AtMTM1 and AtMTM2 show distinct localization patterns inside cells, as only AtMTM1 appears in granulate "punctate structures." It would be of great interest to determine their nature as well as that of the structures associating with AtMTM2.

For the most part, the biological functions of MTMs are still poorly understood, but association with specific membranes is considered critical for their function and loss of this association is linked to various diseases (Skwarek and Boulianne, 2009). The RID domain, conserved in all MTMs, is responsible for the membrane location of MTM1 in human cells (Laporte et al., 2002), and this region is particularly rich in mutations found in various diseases (Begley and Dixon, 2005). In this regard, it is interesting to note the L250W substitution in the RID domain of AtMTM2 resulting in a changed cellular localization of the protein (Fig. 7b–e) as it may provide an example for further studies of the role of RID in MTM function.

Typically, PtdInsPs are studied in the context of their classical roles as second messengers in signal transduction. However, increasing evidence is pointing to an involvement of PtdInsPs in regulating nuclear events as well (Irvine, 2003; Jones and Divecha, 2004; Gozani et al., 2005; Jones et al., 2006). Phosphatidylinositol 5-phosphate binds to the PHD domain of the epigenetic factor ATX1 and negatively regulates its function (Alvarez-Venegas et al., 2006a,b; Ndamukong et al., 2010). Production of PtdIns5P by an active AtMTM1 is required for the cellular localization of ATX1 and a mutation in the AtMTM1 active site that affects its phosphatase activity towards PtdIns(3,5)P_2 failed to retain the ATX1-ePHD in the cytoplasm(Ndamukong et al., 2010). It was found that ATX1 loss-of-function and AtMTM1 over-expressing plants responded similarly to water-deprivation stress. The ATX1 and AtMTM1 proteins co-regulate a common set of genes (Ding et al., 2009), linking ATX1, AtMTM1, and PtdIns5P in a biologically relevant pathway. Importantly, there were only four misregulated genes, and no genes co-regulated with ATX1 during the Arabidopsis response to the stress.

Collectively, our results demonstrate that the two monophyletic, highly conserved Arabidopsis MTM genes have evolved along different functional paths. AtMTM1, but not AtMTM2, participates in the dehydration stress response, regulating the plant's transcriptome and the endogenous levels of PtdIns5P. The role of AtMTM2 remains unclear.

Experimental Procedures

Plant material and selection for AtMTM1 *and* AtMTM2 *insertion lines*

Wild-type and mutant plants were grown in soil under the same controlled daylight environmental conditions (12 h light, 20°C, regular watering). For soil-dehydration stress, watering of 3-week-old plants was terminated for 19 days. Four *Ti*-insertion lines (José et al., 2003) were analyzed for *AtMTM1* function: SALK_135710, SALK_018481, SALK_073312, and SALK_029185. Three were analyzed for *AtMTM2*: SALK_147338, SALK_082030, and SALK_147282. Homozygous mutant lines were selected, verified by genotyping and tested for producing mRNAs (see Table S1 for specific primers).

Constructs

Transgenic plants were generated by transformation with binary vectors. Binary plasmids were transformed into chemically competent *Agrobacterium tumefaciens* strain C58C1 by incubating DNA with agrobacteria on ice for 5 min, freezing in liquid nitrogen for 5 min, and heat shock at 37°C for 5 min. The cells were allowed to recover in growth medium with shaking for 2 h at 20°C and plated on selection medium containing rifampicin, gentamycin, and a third antibiotic for plasmid selection. Agrobacteria selected for transformation were used to transform Col-0 plants using a floral dipping method as described (Clough and Bent, 1998). For cloning approaches, vectors, and primers see the Appendix S1 (Supporting Methods).

Tobacco transient assays

Transient expression of fluorescent tagged proteins was carried out as described before (Ndamukong et al., 2010). Detection of expressed proteins was determined 40 h after *A. tumefaciens* mediated transformation, by laser scanning confocal microscopy using 488- and 633-nm excitation and two-channel measurement of emission, 522 nm (green/GFP), and 680 nm (red/chlorophyll). Red fluorescent protein (RFP) was detected by excitation at 540 nm and emission at 590 nm.

Real-time quantitative RT-PCR analysis

The RNA for quantitative RT-PCR was isolated with TRIZOL (Invitrogen, http://www.invitrogen.com/) and purified with a RNeasy Plant Mini Kit (Qiagen, catalogue number 74903, http://www. qiagen.com/). For first-strand cDNA synthesis 8 μg total RNA was treated with DNase I, extracted with phenol and chloroform, precipitated with ethanol, followed by the addition of oligo (dT) and superscript III reverse transcriptase (Invitrogen). The RT-PCR analysis was performed using the iCycleriQ real-time PCR instrument (Bio-Rad, http://www.bio-rad.com/) and iQ SYBR Green Supermix (Bio-Rad). The relative expression of specific genes was quantified using $2^{-\Delta\Delta Ct}$ calculation, where ΔC_t is the difference in the threshold cycles of the test and housekeeping gene *ACTIN7*. The mean threshold cycle values for the genes of interest were calculated from three experiments.

The PtdIns5P mass assay

The specificity of the reactions and relevant controls were exactly as described earlier for the AtMTM1-overexpressing cells (Ndamukong et al., 2010). Detailed description of the method is in Appendix S1, Supporting Methods.

Phosphatase activity

Phosphoinositide 3-phosphatase assays were performed using the malachite green assay (Martin et al., 1985; Schaletzky et al., 2003) with a standardized phosphatase kit (Echelon K1500 JJ-052208, http://www.echelon-inc.com/) according to the manufacture's protocol. Recombinantly expressed and affinity-column purified GST-tagged proteins were reacted with the Mono- and Di-C8 phosphoinositides (Echelon) as substrates. Phosphatase and tensin (PTEN) lipid phosphatase (Echelon, E-3000) was used as a positive control. Inorganic phosphate release was measured by a standard curve of KH2PO4 in distilled water (Ding et al., 2009).

Microarray analysis

Affymetrix ATH1 Genome Arrays (Affymetrix, http://www.affymetrix. com/) were used for the analysis of expression of ~24 000 Arabidopsis genes in watered and in dehydration-stressed samples of the Col-0 (wild type), *mtm1-1* and *mtm2* mutant backgrounds. All microarray analyses were performed at University of Nebraska at Lincoln's Center for Biotechnology Bioinformatics and Genomics Core Research Facilities (see Appendix S1, Supporting Methods for details).

The gene expression data from the analysis of *mtm1* and *mtm2* have been deposited at the NCBI Gene Expression Omnibus with series number GSE15577.

Acknowledgments – We are grateful to C. Elowski (University of Nebraska at Lincoln) for expert help with the microscopy. The work was partially supported by NSF-MCB0749504 award to Z.A. Research at the Paterson Institute for Cancer Research is entirely funded by Cancer Research UK.

References

Alvarez-Venegas, R., Xia, Y., Lu, G. and Avramova, Z. (2006a) Phosphoinositide 5-Phosphate and Phosphoinositide 4-Phosphate Trigger Distinct Specific Responses of *Arabidopsis* Genes. *Plant Signal. Behav.* 1, 140–151.

Alvarez-Venegas, R., Sadder, M., Hlavacka, A. et al. (2006b) The Arabidopsis homolog of trithorax, ATX1, binds phosphatidylinositol 5-phosphate, and the two regulate a common set of target genes. *Proc. Natl Acad. Sci. USA* 103, 6049–6054.

Avramova, Z. (2009) Evolution and pleiotropy of TRITHORAX function in Arabidopsis. *Int. J. Dev. Biol.* 53, 371–381.

Begley, M.I., and Dixon, J.E. (2005) The structure and regulation of myotubularin phosphatases. *Curr. Opin. Struct. Biol.* 15, 614–620.

Begley, M.J., Taylor, G.S., Kim, S.A., Veine, D.M., Dixon, J.E. and Stuckey, J.A. (2003) Crystal structure of a phosphoinositide phosphatase, MTMR2: insights into myotubular myopathy and Charcot–Marie–Tooth syndrome. *Mol. Cell* 12, 1391–1402.

Begley, M.J., Taylor, G.S., Brock, M.A., Ghosh, P., Woods, V.L. and Dixon, J.E. (2006) Molecular basis for substrate recognition by MTMR2, a myotubularin family phosphoinositide phosphatase. *Proc. Natl Acad. Sci. USA* 103, 927–932.

Beilstein, M.A., Nagalingum, N.S., Clements, M.D., Manchester, S.R. and Mathews, S. (2010) Dated molecular phylogenies indicate a Miocene origin for *Arabidopsis thaliana*. *Proc. Natl Acad. Sci. USA* 107, 18724–18728.

Blondeau, F., Laporte, J., Bodin, S., Superti-Furga, G., Payrastre, B. and Mandel, J.L. (2000) Myotubularin, a phosphatase deficient in myotubular myopathy, acts on phosphatidylinositol 3-kinase and phosphatidylinositol 3-phosphate pathway; *Hum. Mol. Genet.* 9, 2223–2229.

Bolino, A., Muglia, M., Conforti, F.L., et al. (2000) Charcot–Marie–Tooth type 4B is caused by mutations in the gene encoding myotubularin-related protein-2. *Nat. Genet.* 25, 17–19.

Boss, W.F., Davis, A.J., Im, Y.J., Galvão, R.M. and Perera, I.Y. (2006) Phosphoinositide metabolism: towards an understanding of subcellular signaling. *Subcell. Biochem.* 39, 181–205.

Cao, C., Backer, J.M., Laporte, J., Bedrick, E.J. and Wandinger-Ness, A. (2008) Sequential actions of myotubularin lipid phosphatases regulate endosomal PI(3)P and growth factor receptor trafficking. *Mol. Biol. Cell* 19, 3334–3346.

Carlton, J.G., and Cullen, P.J. (2005) Coincidence detection in phosphoinositide signaling. *Trends Cell Biol.* 15, 540–547.

Carricaburu, V., Lamia, K.A., Lo, E., Favereaux, L., Payrastre, B., Cantley, L.C. and Rameh, L.E. (2003) The phosphatidylinositol (PI)-5-phosphate 4-kinase type II enzyme controls insulin signaling by regulating PI-3,4,5-trisphosphate degradation. *Proc. Natl Acad. Sci. USA* 100, 9867–9872.

Cazzonelli, C.I., Millar, T., Finnegan, E.J. and Pogson, B.J. (2009) Promoting gene expression in plants by permissive histone lysine methylation. *Plant Signal. Behav.* 4, 484–488.

Choi, Y., Lee, Y., Jeon, B.W., Staiger, C.J. and Lee, Y. (2008) Phosphatidylinositol 3- and 4-phosphate modulate actin filament reorganization in guard cells of day flower. *Plant, Cell Environ.* 31, 366–377.

Clough, S.J., and Bent, A.F. (1998) Floral dip: a simplified method for Agrobacterium-mediated transformation of *Arabidopsis thaliana*. *Plant J.* 16, 735–743.

Coronas, S., Ramel, D., Pendaries, C., Gaits-Iacovoni, F., Tronchère, H. and Payrastre, B. (2007) PtdIns5P: a little phosphoinositide with big functions? *Biochem. Soc. Symp.* 74, 117–128.

Ding, Y., Lapko, H., Ndamukong, I. et al. (2009) The Arabidopsis chromatin modifier ATX1, the myotubularin-like AtMTM, and the response to drought. *Plant Signal. Behav.* 4, 1049–1058.

Gozani, O., Karuman, P., Jones, D.R. et al. (2004) The PHD finger of the chromatin-associated protein ING2 functions as a nuclear phosphoinisitide receptor. *Cell* 114, 99–111.

Gozani, O., Field, S., Ferguson, C., Ewalt, M., Mahlke, C., Cantley, L.C., Prestwich, G.D. and Yuan, J. (2005) Modification of protein subnuclear localization by synthetic phosphoinositides: evidence for nuclear phosphoinositide signaling mechanisms. *Adv. Enzyme Reg.* 45, 171–185.

Hedges, S.B., Blair, J.E., Venturi, M.L. and Shoe, J.L. (2004) A molecular timescale of eukaryote evolution and the rise of complex multicellular life. *BMC Evol. Biol.* 28, 4.

Herron, M.D., Hackett, J.D., Aylward, F.O. and Michod, R.E. (2009) Triassic origin and early radiation of multicellular volvocine algae. *Proc. Natl Acad. Sci. USA* 106, 3254–3258.

Irvine, R.F. (2003) Nuclear lipid signaling. *Nat. Rev.* 4, 1–12.

Jaillon, O., et al. (2007) The grapevine genome sequence suggests ancestral hexaploidization in major angiosperm phyla. *Nature* 449, 463–467.

Jones, D.R., and Divecha, N. (2004) Linking lipids to chromatin. *Curr. Opin. Genet. Dev.* 14, 196–202.

Jones, D.R., Bultsma, Y., Keune, W.J., Halstead, J.R., Elouarrat, D., Mohammed, S., Heck, A.J., D'Santos, C.S. and Divecha, N. (2006) Nuclear PtdIns5P as a transducer of stress signaling: an in vitro role for PIP4Kbeta. *Mol. Cell* 23, 685–695.

Jones, D.R., Bultsma, Y., Keune, W.J. and Divecha, N. (2009) Methods for the determination of the mass of nuclear PtdIns4P, PtdIns5P, and PtdIns(4,5)P2. *Methods Mol. Biol.* 462, 75–88.

José, M., et al. (2003) Genome-wide insertional mutagenesis of Arabidopsis thaliana. *Science* 301, 653–657.

Jung, J.-Y., Kim, Y.-W., Kwak, J.M., et al. (2002) Phosphatidylinisitiol 3-and 4-phsphate are required for normal stomatal movements. *Plant Cell* 14, 2399–2412.

Kerk, D. and Moorhead, G.B. (2010) A phylogenetic survey of myotubularin genes of eukaryotes: distribution, protein structure, evolution, and gene expression. *BMC Evol. Biol.* 10, 196.

Kim, S.A., Taylor, G.S., Torgersen, K.M. and Dixon, J.E. (2002) Myotubularin and MTMR2, phosphatidylinositol 3-phosphatases mutated in myotubular myopathy and type 4B Charcot–Marie–Tooth disease. *J. Biol. Chem.* 277, 4526–4531.

Kondrashov, F.A., Rogozin, I.B., Wolf, Y.I. and Koonin, E.V. (2005) Selection in the evolution of gene duplication. *Genome Biol.* 2(18), 8.1–8.9.

König, S., Mosblech, A. and Heilmann, I. (2007) Stress-inducible and constitutive phosphoinositide pools have distinctive fatty acid patterns in *A. thaliana*. *FASEB J.* 21, 1958–1967.

König, S., Ischebeck, T., Lerche, J., Stenzel, I. and Heilmann, I. (2008) Salt-stress-induced association of phosphatidylinositol 4,5-bisphosphate with clathrin-coated vesicles in plants. *Biochem J.* 415, 387–399.

Laporte, J., Hu, L.J., Kretz, C., Mandel, J.L., Kioschis, P., Coy, J.F., Klauck, S.M., Poustka, A. and Dahl, N. (1996) A gene mutated in X-linked myotubular myopathy defines a new putative tyrosine phosphatase family conserved in yeast. *Nat. Genet.* 13, 175–182.

Laporte, J., Blondeau, F., Gansmuller, A., Lutz, Y., Vonesch, J.L. and Mandel, J.L. (2002) The PtdIns3P phosphatase myotubularin is a cytoplasmic protein that also localizes to Rac1-inducible plasma membrane ruffles. *J. Cell Sci.* 115, 3105–3117.

Laporte, J., Bedez, F., Bolino, A. and Mandel, J.L. (2003) Myotubularins, a large disease-associated family of cooperating catalytically active and inactive phosphoinositide phosphatases. *Hum. Mol. Genet.* 12, R285–R292.

Lecompte, O., Poch, O. and Laporte, J. (2008) PtdIns5P regulation through evolution: roles in membrane trafficking? *Trends Biochem. Sci.* 33, 453–460.

Martin, B., Pallen, C.J., Wang, J.H. and Graves, D.J. (1985) Use of fluorinated tyrosine phosphates to probe the substrate specificity of the low molecular weight phosphatase activity of calcineurin. *J. Biol. Chem.* 260, 14932–14937.

Meijer, H.J.G. and Munnik, T. (2003) Phospholipid-based signaling in plants. *Annu. Rev. Plant Biol.* 54, 265–306.

Meijer, H.J.G., Berrier, C.P., Iurisci, C., Divecha, N., Musgrave, A. and Munnik, T. (2001) Hyperosmotic stress induces rapid synthesis of phosphatidyl-D-inositol 3,5-bisphosphate in plant cells. *Biochem. J.* 360, 491–498.

Merchant, S.S. et al. (2007) The Chlamydomonas genome reveals the evolution of key animal and plant functions. *Science* 318, 245–250.

Michell, R.H., Heath, V.L., Lemmon, M.A. and Dove, S.K. (2006) Phosphatidylinositol 3,5-bisphosphate: metabolism and cellular functions. *Trends Biochem. Sci.* 31, 52–63.

Munnik, T. and Vermeer, J.E. (2010) Osmotic stress-induced phosphoinositide and inositol phosphate signalling in plants. *Plant, Cell Environ.* 33, 655–669.

Nandukar, H.H., Layton, M.J., Laporte, J., Selan, C., Corcoran, L., Caldwell, J.C., Mochizuki, Y., Majerus, P.W. and Mitchell, C.A. (2003) Identification of myotubularin as the lipid phosphatase catalytic subunit associated with the 3-phosphatase adapter protein, 3-PAP. *Proc. Natl Acad. Sci. USA* 100, 8660–8665.

Ndamukong, I., Jones, D., Lapko, H., Divecha, N. and Avramova, Z. (2010) Phosphatidylinositol 5-phosphate links dehydration stress to the activity of ARABIDOPSIS TRITHORAX-LIKE factor ATX1. *PLoS One* 5(10), e13396.

Niebhur, K., Giuriato, S., Pedron, T., Philpott, D.J., Gaits, F., Sable, J., Sheetz, M.P., Parsot, C., Sansonetti, P.J. and Payrastre, B. (2002) Conversion of PtdIns(4,5)P2 into PtdIns(5)P by the Shigella flexneri effector IpgD reorganizes host cell morphology. *EMBO J.* 21, 5069–5078.

Park, K.Y., Jung, J.Y., Park, J., Hwang, J.U., Kim, Y.W., Hwang, I. and Lee, Y. A role for phosphatidylinositol 3-phosphate in abscisic acid-induced reactive oxygen species generation in guard cells. *Plant Physiology* 132, 92–98.

Pendaries, C., Tronchère, H., Plantavid, M. and Payrastre, B. (2003) Phosphoinositide signaling disorders in human diseases. *FEBS Lett.* 546, 25–31.

Pendaries, C., Tronchère, H., Racaud-Sultan, C., Gaits-Iacovoni, F., Coronas, S., Manenti, S., Gratacap, M.P., Plantavid, M. and Payrastre, B. (2005) Emerging roles of phosphatidylinositol monophosphates in cellular signaling and trafficking. *Adv. Enzyme Regul.* 45, 201–214.

Pical, C., Westergren, T., Dove, S.K., Larsson, C. and Sommarin, M. (1999) Salinity and hyperosmotic stress induce rapid increases in phosphatidylinositol 4,5-bisphosphate, diacylglycerol pyrophosphate and phosphatydylcholine in *Arabidopsis thaliana* cells. *J. Biol. Chem.* 274, 38232–38240.

Pickett, F.B. and Meeks-Wagner, D.R. (1995) Seeing double: appreciating genetic redundancy. *Plant Cell* 7, 1347–1356.

Quatrano, R.S., McDaniel, S.F., Khandelwal, A., Perroud, P.F. and Cove, D.J. (2007) Physcomitrella patens: mosses enter the genomic age. *Curr. Opin. Plant Biol.* 10, 182–189.

Rameh, L., Tolias, K.F., Duckworth, B.C. and Cantley, L.C. (1997) A new pathway for synthesis of phosphatidylinositol 4,5-bisphosphate. *Nature* 390, 192–196.

Robinson, F.L. and Dixon, J. (2006) Myotubularin phosphatases: policing 3-phosphoinositides. *Trends Cell Biol.* 16, 403–412.

Sbrissa, D., Ikonomov, O.C., Deeb, R. and Shisheva, A. (2002) Phosphatidylinositol 5-phosphate biosynthesis is linked to PIKfyve and is involved in osmotic response pathway in mammalian cells. *J. Biol. Chem.* 277, 47276–47284.

Schaletzky, J., Dove, S.K., Short, B., Lorenzo, O., Clague, M.J. and Barr, F.A. (2003) Phosphatidylinositol-5-phosphate activation and conserved substrate specificity of the myotubularin phosphatidylinositol 3-phosphatases. *Curr. Biol.* 13, 504–509.

Skwarek, L.C. and Boulianne, G.L. (2009) Great expectations for PIP: phosphoinositides as regulators of signaling during development and disease. *Dev. Cell* 16, 12–20.

Taylor, G.S., Maehama, T. and Dixon, .E. (2000) Myotubularin, a protein tyrosine phosphatase mutated in myotubular myopathy, dephosphorylates the lipid second messenger, phosphatidylinositol 3-phosphate. *Proc. Natl Acad. Sci. USA* 97, 8910–8915.

Tronchère, H., Laporte, J., Pendaries, C., Chaussade, C., Liaubet, L., Pirola, L., Mandel, J.L. and Payrastre, B. (2004) Production of phosphatidylinositol 5-phosphate by the phosphoinositide 3-phosphatase myotubularin in mammalian cells. *J. Biol. Chem.* 279, 7304–7312.

Tuskan, G.A. et al. (2006) The genome of black cottonwood, *Populus trichocarpa* (Torr. & Gray). *Science* 313, 1596–1604.

Ungewickell, A., Hugge, C., Kisseleva, M., Chang, S.C., Zou, J., Feng, Y., Galyov, E.E., Wilson, M. and Majerus, P.W. (2005) The identification and characterization of two phosphatidyl-inositol-4,5-biphosphate 4-phosphates. *Proc Natl Acad. Sci. USA* 102, 18854–18859.

Vallutu, R. and Van den Ende, W. (2011) *Myo*-inositol and beyond-Emerging networks under stress. *Plant Sci.* 181, 397–400.

Vergne, I. and Deretic, V. (2010) The Role of PI3P Phosphatases in the Regulation of Autophagy. *FEBS Lett.* 584, 1313–1318.

Wang, X. (2004) Lipid signaling. *Curr. Opin. Plant Biol.* 7, 329–336.

Wang, N.N., Shih, M.C. and Li, N. (2005) The GUS reporter-aided analysis of the promoter activities of Arabidopsis ACC synthase genes AtACS4, AtACS5, and AtACS7 induced by hormones and stresses. *J. Exp. Bot.* 56, 909–920.

Zonia, L. and Munnik, T. (2004) Osmotically induced cell swelling versus cell shrinking elicits specific changes in phospholipid signals in tobacco pollen tubes. *Plant Physiol.* 134, 813–823.

SUPPLEMEMNTARY FIGURES

Supplementary Figure 1 (SF 1)

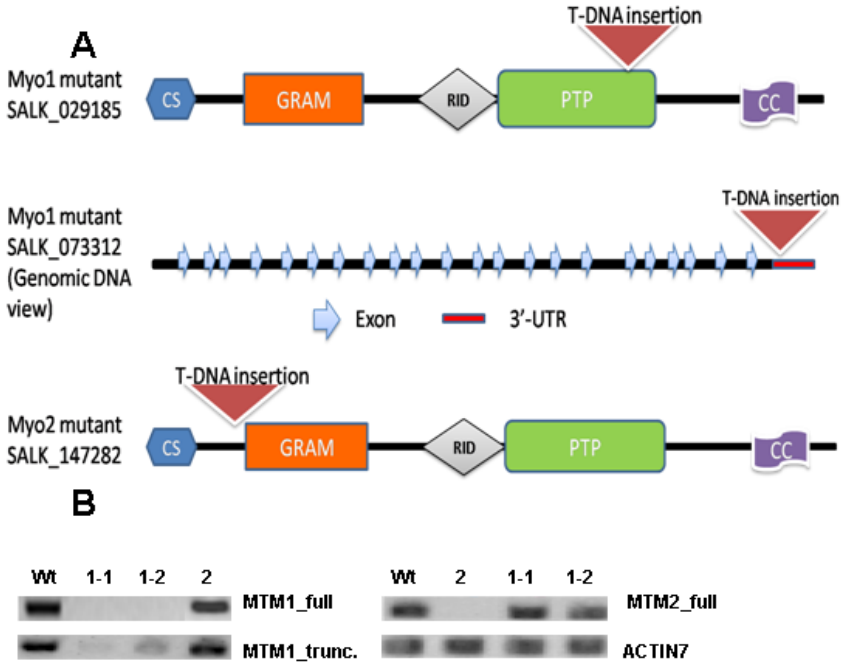

SF 1. *Ti*-Insertion lines for the *AtMTM1* and *AtMTM2* loci

A) Structures of the mutant lines used in this study are shown. The site of the *Ti*-DNA insertion is shown as a red triangle. Line SALK_029185, referred to as the *mtm1-1* mutant; SALK_ 073312, as the *mtm1-2*, and SALK_147282, as *mtm2* mutant, respectively; **B)** Production of full-size, as well as truncated, *AtMTM1* mRNAs in the different genetic backgrounds is shown in the left-hand panels. Production of *AtMTM2* mRNAs in the different genetic backgrounds is shown in the right-hand panel. Actin is included as a loading control. The genetic backgrounds are shown on top of lanes: 1-1 is *mtm1-1*, 1-2 is *mtm1-2*, and 2 is the *mtm2* mutant line. Unique primers were used for detection of full or truncated mRNAs, shown in ST1.

Supplementary Figure 2 (SF 2)

SF 2. Response to soil water-withdrawal of *mtm1-2* mutant plants

Homozygous *mtm1-2* and *mtm1-2¯/mtm2* plants after 19 days without watering.

Supplementary Figure 3 (SF 3)

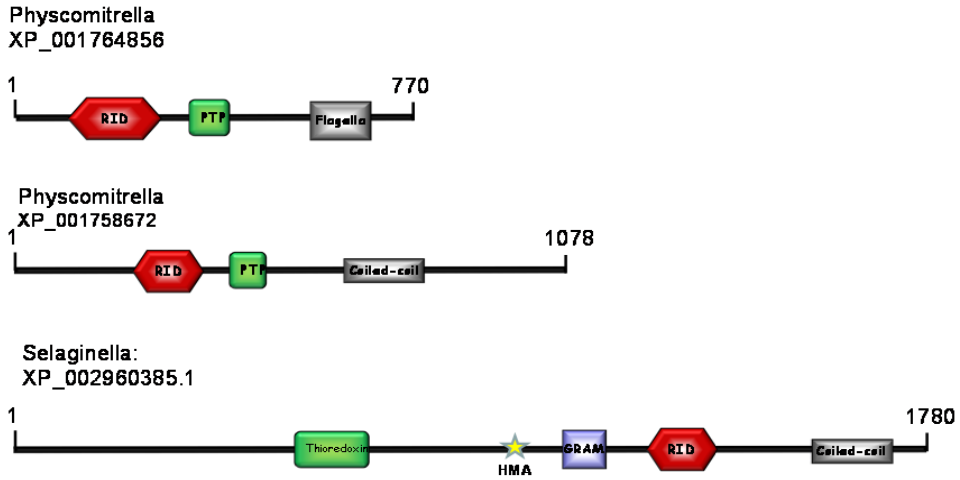

SF 3. Structure of the two myotubularins from the moss (Physcomitrella) and from Selaginella

The two Physcomitrella myotubularins have structures similar to the animal and land plants' proteins. The C-terminal domains of the moss proteins belong to the Flagellar family of proteins found in eukaryotic paraflagellar rod component proteins. The two moss proteins are most highly related to each other supporting a species-specific duplication event. The putative myotubularin from Selaginella contains additional N-terminally located sequences representing a unique combination of domains not seen in other reported species.

SUPPLEMEMNTARY TABLE 1: Primers used for the various cloning and analytical procedures.

Primer	5'-3' Sequence	Purpose
Actin7 qtPCR-Fwd	CTACGAGGGGTATGCTCTTCCTCAT	Forward qT-PCR primer for actin control
Actin7 qtPCR-Rev	CTGAAGAACTGCTCTTGGCTGTCTC	Reverse qT-PCR primer for actin control
ATMTM1 ACTIV F	CAATGAGGGAGAGCTTTTCCCG	Forward primer for PCR Analysis of MTM1
ATMTM1 ACTIV R	AGCCTGAAACCCAGCAAAAGTTC	Reverse primer for PCR Analysis of MTM2
attB1-MTM1-FWD	GGGGACAAGTTTGTACAAAAAAGCAGGC TTAATGACGCCGCCGAGACCACCG	Gateway Forward primer for amplification and cloning of MTM1 cDNA
attB1-MTM2	GGGGACAAGTTTGTACAAAAAAGCAGGC TTAATGACGGCGCTGAGACCT	Gateway Forward primer for amplification and cloning of MTM2 cDNA
attB2 MTM1(no stop)	GGGGACCACTTTGTACAAGAAAGCTGGG TATTTAGGTTGGAAATAGCTATCG	Gateway Reverse primer for amplification and cloning of MTM1 cDNA to C- terminal tags
attB2-MTM2	GGGGACCACTTTGTACAAGAAAGCTGGG TATCATTCAGCTGTGAAATA	Gateway Reverse primer for amplification and cloning of MTM2 cDNA
LBb1	ATTTTGCCGATTTCGGAAC	Salk left border primer for t-DNA insertion mutation analysis
MTM1 RT vs2 F	GATTAACTTCACCACATCTGATGTCG	Forward primer for RT PCR amplification of MTM1 from cDNA
MTM1 RT vs2 R	CCCTTTCGGGTTTCCAGATG	Reverse primer for RT PCR amplification of MTM1 from cDNA
MTM2 RT vs1 F	CACAAGAAACGGAGATTGCACAG	Forward primer for RT PCR amplification of MTM2 from cDNA
MTM2 RT vs1 R	CACACTGCTTCACACACATTTTGTTC	Reverse primer for RT PCR amplification of MTM2 from cDNA
MTM2-PROMOTER-F	ATAAGCTTAGCTGGCCAAGAGAAGA	Cloning the 5' of MTM2 promoter into pCambia via *Hind* III
MTM2-PROMOTER-PST-F	AACTGCAGAGCTGGCCAAGAG	Cloning the 5' of MTM2 promoter into pCambia via *PstI*
MTM2-PROMOTER-R	AACCATGGGTAAAAAAGGAGAGAGA	Cloning the 3' end of the MTM2 promoter into the pCambia vector via *Nco* I
MTM2-UNIQUE1-F	TCACGATCGCTGCGATGTTC	Forward primer for PCR analysis of MTM2
MTM2-UNIQUE2-R	CATATGAAGAGCTAGAGGATTGAGCA	Reverse primer for PCR analysis of MTM2
RBprimer	ATCGATGGGGTTAAGAAAG	Salk Right border primer for t-DNA insertion mutation analysis
Salk_018432 LP	TCTGCCAACCCATTGAAATAG	Left primer for analysis of Salk_018432
Salk_018432 RP	GATGGGAGATCATCGTTCTTG	Right primer for analysis of Salk_018432
Salk_018481 LP	TCTGCCAACCCATTGAAATAG	Left primer for analysis of Salk_018481
Salk_018481 RP	GATGGGAGATCATCGTTCTTG	Right primer for analysis of Salk_018481
Salk_029185 LP	GCTGTGAAACGCTATCAATCC	Left primer for analysis of Salk_029185
Salk_029185 RP	TGTGAATTCTGCAGAGACACG	Right primer for analysis of Salk_029185
Salk_073312 LP	TCACTCGGGTGCAAGATTAAC	Left primer for analysis of Salk_073312
Salk_073312 RP	CGTAGGTTTCTTCTCCGATCC	Right primer for analysis of Salk_073312
Salk_147282 LP	TTTTATGAAAAAGAGACAAATTTCC	Left primer for analysis of Salk_147282
Salk_147282 RP	CAAGTGGAACAAGCTTTCTGG	Right primer for analysis of Salk_147282

SUPPLEMENTARY TABLE 2 (ST2): Genes with up-regulated or down-regulated transcription in the *mtm1* mutant background *versus* Col0 in the watered state

Signal log Ratio	Gene	Encoded protein
2.491	AT1G12710	AtPP2-A12 (Phloem protein 2-A12); carbohydrate binding
2.128	AT1G27630	CYCT1;3 (CYCLIN T 1;3); cyclin-dependent protein kinase
2.392	AT2G39900	LIM domain-containing protein
1.603	AT3G10410	scpl49 (serine carboxypeptidase-like 49); serine-type carboxypeptidase
1.459	AT3G15840	PIFI (post-illumination chlorophyll fluorescence increase)
1.504	AT3G50210	2-oxoacid-dependent oxidase, putative
4.204	AT4G04330	unknown protein
2.669	AT4G30660	hydrophobic protein, putative / low temperature and salt responsive protein, putative
2.27	AT4G33490	aspartic-type endopeptidase
1.306	AT5G06610	unknown protein
2.416	AT5G14550	unknown protein
3.612	AT5G24470	APRR5 (ARABIDOPSIS PSEUDO-RESPONSE REGULATOR 5); transcription regulator/ two-component response regulator
1.949	AT5G27280	zinc finger (DNL type) family protein
2.828	AT5G39410	binding / catalytic
1.196	AT5G51550	EXL3 (EXORDIUM LIKE 3)
2.205	AT5G62720	integral membrane HPP family protein
2.547	AT5G64860	DPE1 (DISPROPORTIONATING ENZYME); 4-alpha-glucanotransferase/ catalytic/ cation binding
-2.221	AT1G69160	unknown protein
-1.058	AT1G69570	Dof-type zinc finger domain-containing protein
-3.689	AT2G41250	haloacid dehalogenase-like hydrolase family protein
-2.959	AT3G12580	HSP70 (heat shock protein 70); ATP binding
-2.498	AT3G15310	transposable element gene
-2.655	AT3G47420	glycerol-3-phosphate transporter, putative / glycerol 3-phosphate permease, putative
-2.364	AT4G00050	UNE10 (unfertilized embryo sac 10); DNA binding / transcription factor
-2.041	AT4G15550	IAGLU (INDOLE-3-ACETATE BETA-D-GLUCOSYLTRANSFERASE); UDP-glycosyltransferase/ transferase, transferring glycosyl groups
-1.752	AT5G10930	CIPK5 (CBL-INTERACTING PROTEIN KINASE 5); ATP binding / kinase/ protein kinase/ protein serine/threonine kinase
-3.65	AT5G52570	BETA-OHASE 2 (BETA-CAROTENE HYDROXYLASE 2); carotene beta-ring hydroxylase

SUPPLEMENTARY TABLE 3: Genes with up- or down-regulated transcription in the *mtm1* mutant background in response to dehydration stress*

Signal log Ratio	Gene	Encoded protein
4.812	AT4G04330	unknown protein
4.788	AT2G21660	CCR2 (COLD, CIRCADIAN RHYTHM, AND RNA BINDING 2); RNA binding / double-stranded DNA binding / single-stranded DNA binding
4.528	AT3G22830	AT-HSFA6B; DNA binding / transcription factor
4.112	AT4G30650	hydrophobic protein, putative / low temperature and salt responsive protein, putative
3.927	AT4G33980	unknown protein
3.539	AT5G48250	zinc finger (B-box type) family protein
3.528	AT5G42900	unknown protein
3.062	AT1G06460	ACD32.1 (ALPHA-CRYSTALLIN DOMAIN 32.1)
2.993	AT3G46640	PCL1 (PHYTOCLOCK 1); DNA binding / transcription factor
2.986	AT4G26670	mitochondrial import inner membrane translocase subunit Tim17/Tim22/Tim23 family protein
2.937	AT3G04550	unknown protein
2.915	AT4G39260	GR-RBP8; RNA binding / nucleic acid binding / nucleotide binding
2.899	AT5G60100	APRR3 (ARABIDOPSIS PSEUDO-RESPONSE REGULATOR 3); transcription regulator/ two-component response regulator
2.843	AT1G69830	AMY3 (ALPHA-AMYLASE-LIKE 3); alpha-amylase
2.783	AT4G32340	
2.773	AT2G40350	DNA binding / transcription factor
2.605	AT1G28050	zinc finger (B-box type) family protein
2.553	AT1G13270	MAP1C (METHIONINE AMINOPEPTIDASE 1B); aminopeptidase/ metalloexopeptidase
2.552	AT5G61380	TOC1 (TIMING OF CAB EXPRESSION 1); transcription regulator/ two-component response regulator
2.494	AT3G07650	COL9 (CONSTANS-LIKE 9); transcription factor/ zinc ion binding
2.488	AT4G09020	ISA3 (ISOAMYLASE 3); alpha-amylase/ isoamylase
2.408	AT3G22240	unknown protein
2.389	AT5G11150	ATVAMP713 (VESICLE-ASSOCIATED MEMBRANE PROTEIN 713)
2.347	AT5G62720	integral membrane HPP family protein
2.3	AT1G17665	unknown protein
2.213	AT3G60530	zinc finger (GATA type) family protein
2.201	AT4G16740	ATTPS03; (E)-beta-ocimene synthase/ myrcene synthase
2.144	AT3G02630	acyl-(acyl-carrier-protein) desaturase, putative / stearoyl-ACP desaturase, putative
2.108	AT4G18930	cyclic phosphodiesterase
2.063	AT5G64860	DPE1 (DISPROPORTIONATING ENZYME); 4-alpha-glucanotransferase/ catalytic/ cation binding
2.055	AT1G59990	DEAD/DEAH box helicase, putative (RH22)
2.054	AT5G50160	FRO8 (FERRIC REDUCTION OXIDASE 8); ferric-chelate reductase/ oxidoreductase
1.989	AT5G58600	PMR5 (POWDERY MILDEW RESISTANT 5)
1.981	AT5G51550	EXL3 (EXORDIUM LIKE 3)
1.961	AT1G22070	TGA3; DNA binding / calmodulin binding / protein binding / transcription factor

1.934	AT1G10200	WLIM1; transcription factor/ zinc ion binding
1.918	AT1G12710	AtPP2-A12 (Phloem protein 2-A12); carbohydrate binding
1.87	AT5G14550	unknown protein
1.867	AT1G17460	TRFL3 (TRF-LIKE 3); DNA binding / transcription factor
1.818	AT1G20020	FNR2 (FERREDOXIN-NADP(+)-OXIDOREDUCTASE 2); NADPH dehydrogenase/ oxidoreductase/ poly(U) binding
1.803	AT4G26130	unknown protein
1.771	AT1G06470	phosphate translocator-related
1.75	AT1G20693	HMGB2 (HIGH MOBILITY GROUP B 2); DNA binding / chromatin binding / structural constituent of chromatin / transcription factor
1.738	AT2G02100	LCR69 (LOW-MOLECULAR-WEIGHT CYSTEINE-RICH 69); peptidase inhibitor
1.733	AT5G01200	myb family transcription factor
1.676	AT1G32860	glycosyl hydrolase family 17 protein
1.671	AT4G20890	TUB9; GTP binding / GTPase/ structural molecule
1.657	AT3G26780	catalytic
1.6	AT2G30870	GSTF10 (HALIANA GLUTATHIONE S-TRANSFERASE PHI 10); copper ion binding / glutathione binding / glutathione transferase
1.577	AT1G34130	STT3B (staurosporin and temperature sensitive 3-like b); oligosaccharyl transferase
1.561	AT3G15840	PIFI (post-illumination chlorophyll fluorescence increase)
1.548	AT5G51350	leucine-rich repeat transmembrane protein kinase, putative
1.513	AT3G28940	avirulence-responsive protein, putative / avirulence induced gene (AIG) protein, putative
1.506	AT5G65080	MAF5 (MADS AFFECTING FLOWERING 5); transcription factor
1.476	AT1G27130	ATGSTU13 (ARABIDOPSIS THALIANA GLUTATHIONE S-TRANSFERASE TAU 13); glutathione transferase
1.437	AT4G38520	protein phosphatase 2C family protein / PP2C family protein
1.39	AT5G08380	AtAGAL1 (Arabidopsis thaliana ALPHA-GALACTOSIDASE 1); alpha-galactosidase/ catalytic/ hydrolase, hydrolyzing O-glycosyl compounds
1.358	AT1G21600	PTAC6 (PLASTID TRANSCRIPTIONALLY ACTIVE6)
1.351	AT1G13000	unknown protein
1.343	AT1G63830	proline-rich family protein
1.338	AT1G48920	ATNUC-L1; nucleic acid binding / nucleotide binding
1.273	AT2G29760	pentatricopeptide (PPR) repeat-containing protein
1.27	AT3G07630	ADT2 (arogenate dehydratase 2); arogenate dehydratase/ prephenate dehydratase
1.247	AT3G62750	BGLU8 (BETA GLUCOSIDASE 8); catalytic/ cation binding / hydrolase, hydrolyzing O-glycosyl compounds
1.243	AT1G12050	fumarylacetoacetase, putative
1.226	AT4G21150	HAP6 (HAPLESS 6); dolichyl-diphosphooligosaccharide-protein glycotransferase
1.221	AT3G17020	universal stress protein (USP) family protein
1.123	AT5G60640	ATPDIL1-4 (PDI-LIKE 1-4); protein disulfide isomerase
1.066	AT5G26880	tRNA/rRNA methyltransferase (SpoU) family protein
1.043	AT4G31040	proton extrusion protein-related
1.042	AT2G36250	FTSZ2-1; protein binding / structural molecule
1.009	AT5G19540	unknown protein
1.005	AT1G06760	histone H1, putative
1	AT3G50440	MES10 (METHYL ESTERASE 10); hydrolase/ hydrolase, acting on ester bonds / methyl jasmonate esterase

-5.037	AT2G46830	CCA1 (CIRCADIAN CLOCK ASSOCIATED 1); DNA binding / transcription activator/ transcription factor/ transcription repressor
-4.767	AT1G01060	LHY (LATE ELONGATED HYPOCOTYL); DNA binding / transcription factor
-4.293	AT1G64500	glutaredoxin family protein
-3.566	AT3G46230	ATHSP17.4
-3.542	AT3G09600	myb family transcription factor
-3.503	AT5G12030	AT-HSP17.6A (ARABIDOPSIS THALIANA HEAT SHOCK PROTEIN 17.6A); unfolded protein binding
-3.362	AT5G09930	ATGCN2; transporter
-3.234	AT3G12320	unknown protein
-3.048	AT1G01520	myb family transcription factor
-3.036	AT2G41250	haloacid dehalogenase-like hydrolase family protein
-2.903	AT5G04380	S-adenosyl-L-methionine:carboxyl methyltransferase family protein
-2.884	AT5G15850	COL1 (constans-like 1); transcription factor/ zinc ion binding
-2.852	AT2G46790	APRR9 (ARABIDOPSIS PSEUDO-RESPONSE REGULATOR 9); protein binding / transcription regulator/ two-component response regulator
-2.817	AT5G06980	unknown protein
-2.784	AT1G52560	26.5 kDa class I small heat shock protein-like (HSP26.5-P)
-2.673	AT2G31380	STH; protein domain specific binding / transcription factor/ zinc ion binding
-2.664	AT1G75100	JAC1 (J-DOMAIN PROTEIN REQUIRED FOR CHLOROPLAST ACCUMULATION RESPONSE 1); heat shock protein binding
-2.62	AT2G22240	MIPS2 (MYO-INOSITOL-1-PHOSTPATE SYNTHASE 2); binding / catalytic/ inositol-3-phosphate synthase
-2.491	AT5G24120	SIGE (SIGMA FACTOR E); DNA binding / DNA-directed RNA polymerase/ sigma factor/ transcription factor
-2.363	AT1G07500	unknown protein
-2.352	AT4G16985	---
-2.254	AT3G10910	zinc finger (C3HC4-type RING finger) family protein
-2.251	AT1G66130	oxidoreductase N-terminal domain-containing protein
-2.25	AT3G28210	PMZ; zinc ion binding
-2.117	AT5G59750	riboflavin biosynthesis protein, putative
-2.116	AT2G33520	
-2.101	AT3G17510	CIPK1 (CBL-INTERACTING PROTEIN KINASE 1); kinase/ protein binding
-2.043	AT4G12400	stress-inducible protein, putative
-2.022	AT1G72760	protein kinase family protein
-2.005	AT4G34250	KCS16 (3-KETOACYL-COA SYNTHASE 16); acyltransferase/ catalytic/ transferase, transferring acyl groups other than amino-acyl groups
-1.973	AT2G02060	transcription factor
-1.94	AT1G48100	glycoside hydrolase family 28 protein / polygalacturonase (pectinase) family protein
-1.917	AT1G12370	PHR1 (PHOTOLYASE 1); DNA photolyase
-1.814	AT4G34610	BLH6 (BELL1-LIKE HOMEODOMAIN 6); DNA binding / transcription factor
-1.794	AT3G21660	UBX domain-containing protein
-1.788	AT3G47420	glycerol-3-phosphate transporter, putative / glycerol 3-phosphate permease, putative
-1.781	AT1G73480	hydrolase, alpha/beta fold family protein

-1.758	AT2G38640	unknown protein
-1.732	AT4G38960	zinc finger (B-box type) family protein
-1.68	AT1G66330	senescence-associated family protein
-1.663	AT2G26800	hydroxymethylglutaryl-CoA lyase, putative / 3-hydroxy-3-methylglutarate-CoA lyase, putative / HMG-CoA lyase, putative
-1.619	AT1G10740	unknown protein
-1.613	AT4G20070	ATAAH (Arabidopsis thaliana Allantoate Amidohydrolase); allantoate deiminase/ metallopeptidase
-1.598	AT2G25680	MOT1 (molybdate transporter 1); molybdate ion transmembrane transporter/ sulfate transmembrane transporter
-1.54	AT1G69570	Dof-type zinc finger domain-containing protein
-1.537	AT2G32150	haloacid dehalogenase-like hydrolase family protein
-1.519	AT1G69480	EXS family protein / ERD1/XPR1/SYG1 family protein
-1.466	AT3G62380	
-1.436	AT3G19270	CYP707A4; (+)-abscisic acid 8'-hydroxylase/ oxygen binding
-1.43	AT3G24170	ATGR1 (glutathione-disulfide reductase); FAD binding / NADP or NADPH binding / glutathione-disulfide reductase/ oxidoreductase
-1.43	AT5G01820	ATSR1 (ARABIDOPSIS THALIANA SERINE/THREONINE PROTEIN KINASE 1); ATP binding / kinase/ protein kinase/ protein serine/threonine kinase
-1.424	AT5G49730	ATFRO6 (FERRIC REDUCTION OXIDASE 6); ferric-chelate reductase/ oxidoreductase
-1.355	AT4G04490	protein kinase family protein
-1.344	AT1G23200	pectinesterase family protein
-1.318	AT5G54470	zinc finger (B-box type) family protein
-1.296	AT1G72100	late embryogenesis abundant domain-containing protein / LEA domain-containing protein
-1.29	AT2G38250	DNA-binding protein-related
-1.203	AT1G74310	ATHSP101 (ARABIDOPSIS THALIANA HEAT SHOCK PROTEIN 101); ATP binding / ATPase/ nucleoside-triphosphatase/ nucleotide binding / protein binding
-1.138	AT4G26200	ACS7; 1-aminocyclopropane-1-carboxylate synthase
-1.092	AT2G46950	CYP709B2; electron carrier/ heme binding / iron ion binding / monooxygenase/ oxygen binding
-1.053	AT3G55580	regulator of chromosome condensation (RCC1) family protein
-1.052	AT1G14490	DNA-binding protein-related

* The signal log ratio is computed versus the values displayed by the Col0 sample under stress

Supplementary Methods. Detailed description of the constructs used, of the PtdIns5P mass assay and the Microarray analyses.

SUPPLEMENTARY METHODS

Constructs: Gateway PCR products were cloned into the entry vector pDONR221 and the entry clones recombined into expression vectors pB7FWG2,0 (Karimi et al., 2002) for C-terminal GFP-fusion and expression in plants; pDESTT17 (Invitrogen) for N-terminal fusion to a 6X his tag and inducible expression in bacteria. A 1440bp and an 880bp promoter PCR fragment were amplified from the AtMTM1 and AtMTM2 promoters respectively, using genomic DNA as a template and PCR specific primers (see ST1). The PCR products were sub-cloned into pGEM-T easy vectors and after confirmation of the correct sequence, were sub-cloned into the pCambia vector, within the *Pst*I and *Nco*I sites. Correct promoter fusions to the GUS reporter in this vector were transformed into *Agrobacteria tumefaciens*, and used to transform *Arabidopsis* to generate transgenic plants. About two dozen transgenic lines expressing GUS under the control of the AtMTM1 promoter or the AtMTM1 promoter were analyzed.

PtdIns5*P* mass assay: Total lipids were extracted from leaves using chloroform (250 μl), methanol (500 μl) and a UCD-200TM bioruptor (Tosho Denki Co., Japan) operating at full power for 2 minutes. After storage at -20°C overnight another round of sonication ensured complete leaf tissue disruption. Water (250 μl), 2.4 M HCl (200 μl) and chloroform (250 μl) were subsequently added to induce phase separation. After thorough mixing and centrifugation (5,000x *g* for 2 minutes at room temperature), the lower chloroform phase was washed once with theoretical upper phase and then dried in a speedvac at room temperature. Neomycin-coated glass bead affinity chromatography was used to selectively purify (yield > 90%) PtdIns*P*s (including PtdIns5*P*) from the total lipid extract (Schacht 1978).

PtdIns5*P* (within the PtdIns*P* fraction) was quantitatively converted into PtdIns(4,5)P_2 using high-specific activity GST-PIP4Kα (1-2μg) in the presence of $MgCl_2$ (10mM final concentration) phosphatidylserine (10nmoles, Sigma), non-radiolabeled ATP (20μM final concentration) and γ^{32}P ATP (10μCi) (Perkin Elmer) in a final volume of 100μl 50mM Tris-HCl pH 7.4 overnight at 30°C with continuous shaking. After total lipid extraction ^{32}P-labelled PtdIns(4,5)P_2 was separated from all other ^{32}P-labelled contaminants using thin layer chromatography. The thin layer chromatography plate was developed once in chloroform/methanol/25% ammonia/water (ratio: 45/35/2/8, v/v/v/v). After air-drying for 30 minutes at room temperature the plate was exposed to a phosphorimaging screen. The amount of ^{32}P-labelled PtdIns(4,5)P_2 generated is directly proportional to the starting mass of PtdIns5*P* in the original sample. A standard curve (0-80pmoles) of PtdIns5*P* (Echelon) phosphorylation in the presence of phosphatidylserine (10nmoles) was always included within individual experiments. PtdIns5*P* mass (pmoles) was normalized according to the starting leaf mass (mg).

Microarray Analysis: Fifteen micrograms of total RNA was used to synthesize cDNA using an Affymetrix One-Cycle cDNA Synthesis Kit according to the manufacturer's instructions. All sample preparations followed prescribed protocols (Affymetrix Genechip Expression Analysis Technical manual). Hybridization was performed at 45°C overnight on the Affymetrix ATH1 Genome Array, stained with streptavidin-phycoerythrin conjugate on an Affymetrix Fluidics Station 450, which was followed by scanning with the GeneChip Scanner 3000 7G (Affymetrix). Affymetrix GeneChip Operating Software (GCOS v1.3) was used for washing, scanning, and basic data analysis. This included calculation of absolute values and normalization of the data with respect to internal standards. Differentially expressed genes between mutant and condition

replicates were determined using the linear models for microarrays package in R/Bioconductor, with Benjamini-Hochberg adjusted p-values (Benjamini and Hochberg, 1995) Genes that were two-fold up- or down-regulated and had a False Discovery Rate adjusted p-value of 0.05 or less were deemed to be significant.

REFERENCES

Benjamini, Y. and Hochberg, Y. (1995) Controlling the false discovery rate: A practical and powerful approach to multiple hypothesis testing. *J. R. Stat. Soc. B* **57,** 289–300.

Karimi, M., Inze, D., Depicker, A. (2002) Gateway vectors for Agrobacterium-mediated plant transformation. *Trends Plant Sci.* **7,** 193-195.

Schacht, J. (1978) Purification of polyphosphoinositides by chromatography on immobilized neomycin. *J. Lipid Res.* 19**,** 1063-1067.